Hindawi Publishing Corporation
Active and Passive Electronic Components
Volume 2015, Article ID 591986, 9 pages
http://dx.doi.org/10.1155/2015/591986

Research Article

A High Efficiency Li-Ion Battery LDO-Based Charger for Portable Application

Youssef Ziadi and Hassan Qjidaa

CED-ST, LESSI, Faculty of Sciences Dhar el Mahraz, Sidi Mohamed Ben Abdellah University, BP 1796, 30003 Fez, Morocco

Correspondence should be addressed to Youssef Ziadi; youssef.ziadi@usmba.ac.ma

Received 2 June 2015; Revised 2 August 2015; Accepted 12 August 2015

Academic Editor: Yuh-Shyan Hwang

This paper presents a high efficiency Li-ion battery LDO-based charger IC which adopted a three-mode control: trickle constant current, fast constant current, and constant voltage modes. The criteria of the proposed Li-ion battery charger, including high accuracy, high efficiency, and low size area, are of high importance. The simulation results provide the trickle current of 116 mA, maximum charging current of 448 mA, and charging voltage of 4.21 V at the power supply of 4.8–5 V, using 0.18 μm CMOS technology.

1. Introduction

As we know, portable devices have become the main applications of advanced technical products. Due to their small size, light weight, and recharge ability, Li-ion batteries are well suited to portable electronic manufactures such as cell phones and PDAs [1] because of their high energy density, long cycle life, high voltage, and absence of memory effects. But the life of a rechargeable battery depends not only on charging time, but also on overcharging control and charging strategies [2]. To avoid the battery from overcharging, the charging process needs a specific method supporting the constant current (CC) and the constant voltage (CV) modes in order to charge the battery by a degrading current [3–5].

In literature, there are several architectures of battery chargers with different approaches of power control methods in order to adapt the supply voltage. The same are characterized by high efficiency such as the DC/DC converter, switching-capacitor, or switching mode power supply [1, 6–8], but they are not suitable for single chip integration and, sometimes, they have low accuracy despite their efficiency. On the other hand, the same are using charge pump as an adaptive supply voltage [3]; however this one is distinguished by its high current ripple and low efficiency. LDO-based charger is characterized by a low current ripple and it can be integrated into the chip without descript components [9], but its major problem is the low efficiency. In this work we will improve the efficiency of an LDO-based charger, using the power transistor as a variable current source and minimizing its dropout.

One of the important missed criteria in several works [1, 3, 6, 8–12] is the control of temperature during charging and the lack of trickle current charge mode in [1, 13] which is necessary for the battery protection when it is fully discharged. That makes this work a complete battery charger chip with respect to all charge procedures and the battery protection.

This paper describes the architecture and simulation results of a three-mode control high efficiency battery charger integrated circuit for Li-ion batteries with charging currents from 116 mA up to 448 mA. In Section 2 we describe the typical charging method of Li-ion battery. The architecture and the functionality of major blocks of the proposed integrated circuit are illustrated in Section 3. Simulation results are shown in Section 4. Finally, the conclusion is remarked in Section 5.

2. Li-Ion Battery Charger Method

Amongst the important criteria of Li-ion battery charger is safety of charging. Yet there are some limitations for the

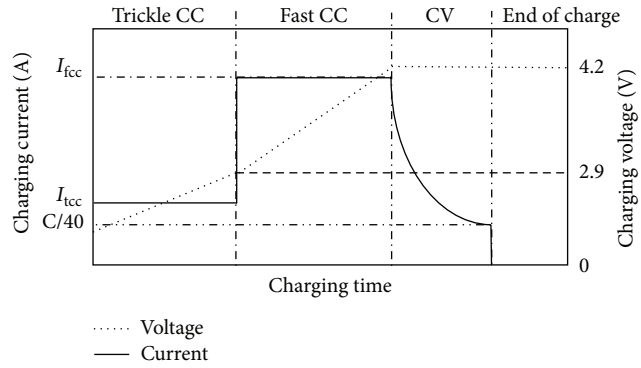

Figure 1: Typical charging process of a Li-ion battery.

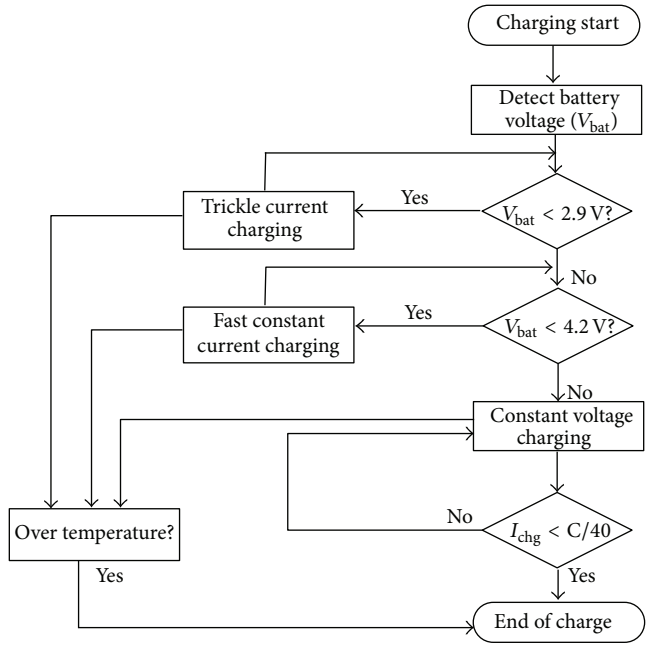

Figure 2: Battery charging flowchart.

current and voltage of charging; thus, the battery temperature will augment severely causing fatal troubles due to some of these limitations.

Notably, the typical charging current is 1C, in which the current can completely charge a battery in one hour [14].

The typical charging profile of Li-ion batteries shown in Figure 1 is needed to achieve three fundamental modes: trickle constant current, fast constant current, and constant voltage modes.

So far as the first trickle constant current mode is concerned, when the battery voltage (V_{bat}) is less than 2.9 V, the internal resistance of Li-ion battery is getting larger; the Li-ion battery, accordingly, has to be charged by a trickle constant current phase; this strategy is called an "overnight charger" [15]; as for the second phase, once the value of V_{bat} is larger than 2.9 V, the process switches from the trickle current to the fast constant current phase.

Ultimately, we use constant voltage to charge the battery when the battery voltage is greater than 4.2 V, whilst the charger is operating within constant voltage mode.

There are two methods to terminate the charging process, the first of which is monitoring the minimum charging current at the CV stage. The charger terminates the charging process when the charging current shrinks to the specified range. To finish the charging process, the other one is based on the maximum charging time [16].

In the proposed design, we have adopted the first method to terminate the charging process; the battery is charging until the charging current is less than 1C/40.

The whole charging flow of our Li-ion battery charger is designed as shown in Figure 2.

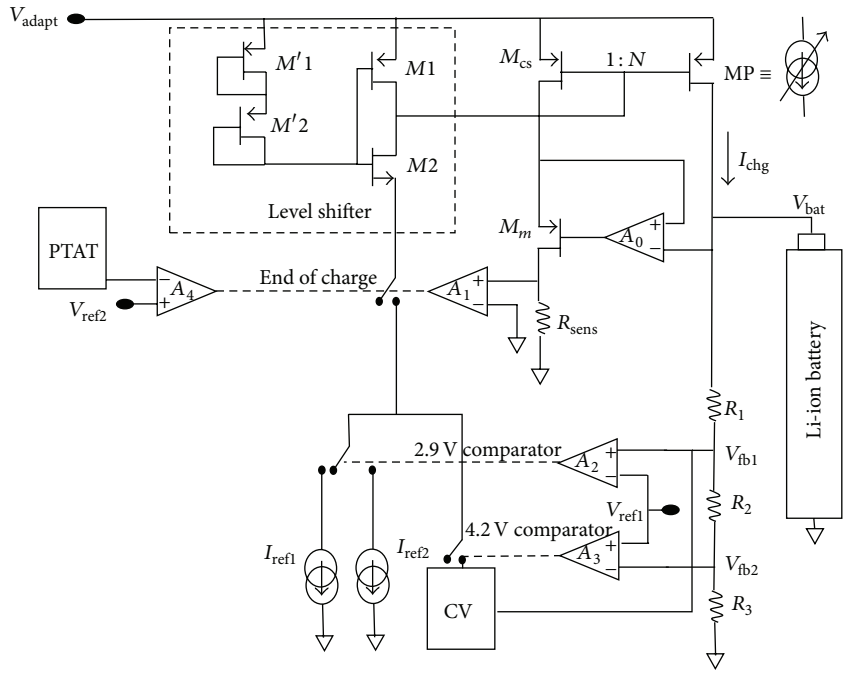

Figure 3: Simplified diagram of the proposed Li-ion battery charger.

3. Circuit Descriptions

Contrary to the other architectures which use a microprocessor to control the different modes of the charge, our proposed architecture is a purely analogic support of the three modes of Li-ion battery charging, trickle constant current, fast constant currant, and constant voltage, as shown in Figure 3. It is made of many blocks: LDO, current generator, current sense, temperature sense (PTAT circuit), and bandgap multioutput. The supplying tension 4.8 V–5 V is adapted by LDO regulator before generating V_{adapt}. The power transistor MP is equivalent to a variable current source; this technique has been used in [10] with flyback converter. The MP control made by two current sources I_{ref1} and I_{ref2} passed through a shifter level composed of $M1$, $M2$, $M'1$, and $M'2$, so that the transistor MP provides a constant current order of 116 mA and 448 mA to order the trickle constant current and the fast constant current modes. We use the integrator to control the constant voltage mode. These modes are switched by Op A_2 and A_3 that compares tensions V_{fb1} and V_{fb2} with V_{ref1}. We use the output of A_1 and A_4 to stop charging when the battery is full or when the temperature detected by the PTAT circuit exceeds 115 degrees.

Figure 4 shows the complete architecture of the proposed Li-ion battery charger. What distinguishes our architecture is the use of current like a parameter of command to switch the power transistor MP between different modes of charge, and it is utilized like a variable current source. The current generator furnishes two reference currents I_{ref1} and I_{ref2} which are copied by current mirror ($M4$ and $M3$) to command the MP gate with level shifter (this current generator will be discussed in Section 3.1). Unlike trickle constant current and fast constant current (CC mode) witch are under the control of I_{ref1} and I_{ref2}, CV mode is controlled by an integrator, following its principles [10]; when V_{fb1} is getting larger gradually, the integrator output is decreasing, so the MP furnishes a current decrease until the end of charge; we could make use of voltage-to-current conversion to generate CV current.

The end of charge occurs when the current sense detects that I_{chg} (charge current) equals 20 mA or when the die temperature transpasses 115°C switching off PMOS (M_{eoc}) integrated into the current generator.

3.1. Current Generator. The current generator furnishes the reference currents, I_{ref1} and I_{ref2}, to control the trickle CC and fast CC modes. We have opted for utilizing this architecture, as shown in Figure 5, which is not influenced by the temperature variation [17]. It is formed by a conventional architecture ($M6$-$M6$-$M9$-$M10$) where the passive resistor is changed with a PMOS transistor $M18$ and its gate bias generator. There are two diode-connected NMOS transistors and one PMOS transistor that make up the gate bias generator, for each mode ($M11$, $M12$, and $M7$ for I_{ref1} mode and $M13$, $M14$, and $M8$ for I_{ref2} mode). Whereas $M7$ copies the reference current I, the gate voltage of $M18$ is generated by the diode-connected transistors $M11$ and $M12$ to generate I_{ref1}. We can generate the reference current I_{ref1} or I_{ref2} by the control switches $M15$ and $M16$. We integrate a transistor M_{eoc} switcher to cancel the generation of I_{ref1} and I_{ref2} to end the charging process.

3.2. Bandgap Reference Multioutput. In our proposed design, four reference tensions would be prerequisite (V_{ref1}, V_{ref2},

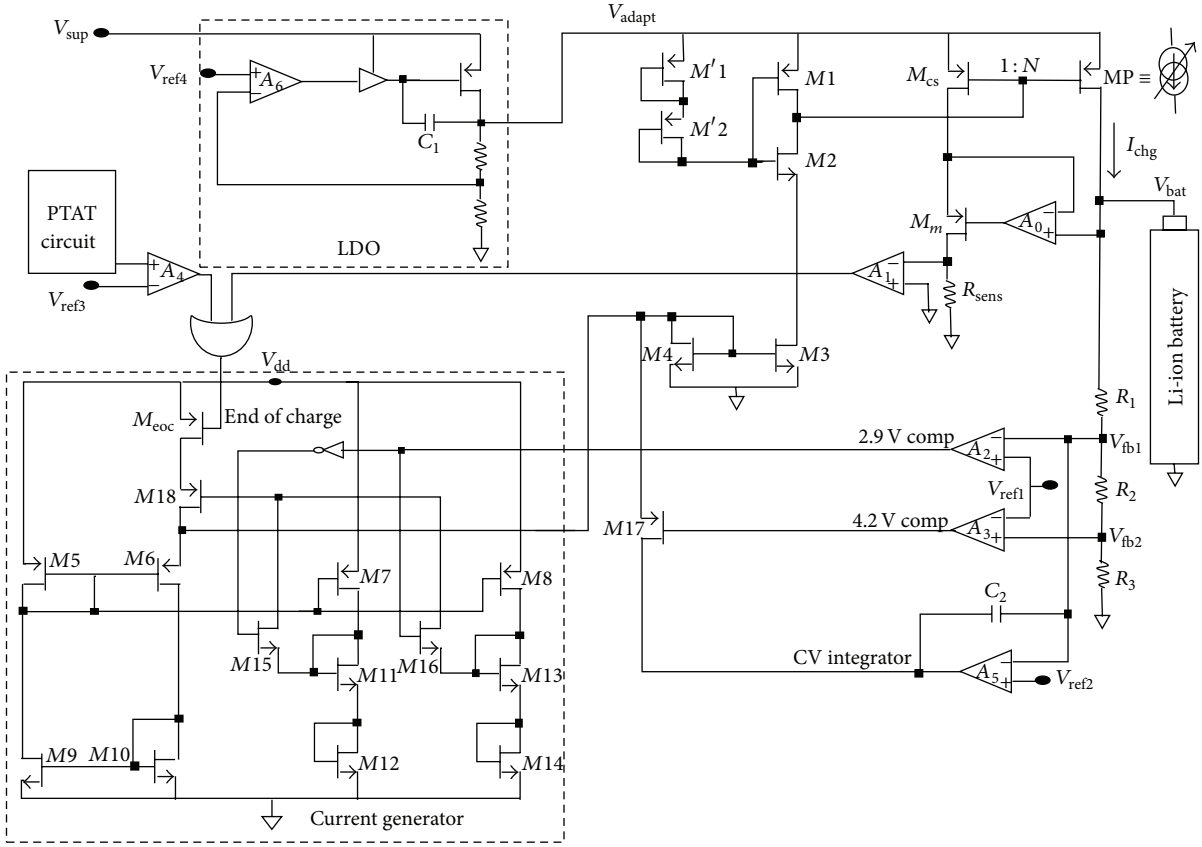

Figure 4: Complete architecture of the proposed Li-ion battery charger.

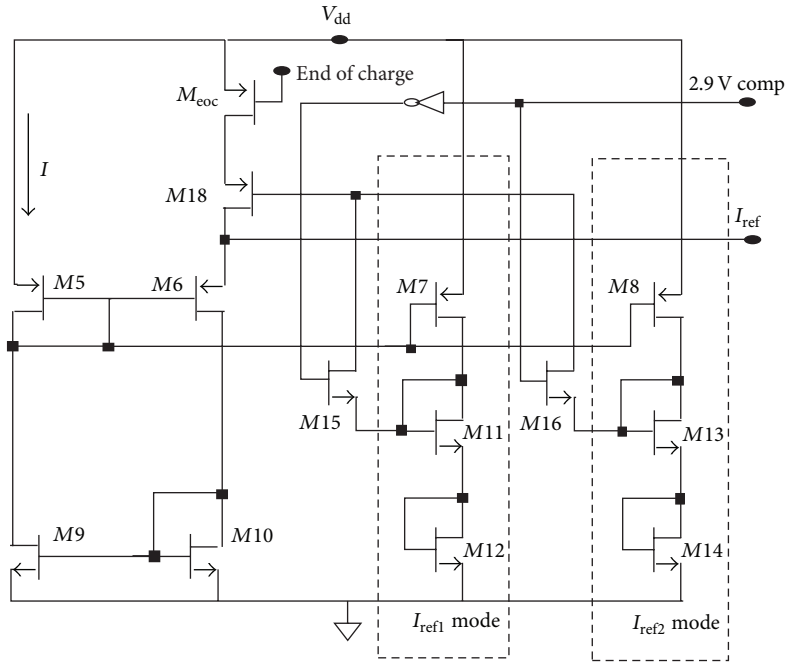

Figure 5: Current generator circuit.

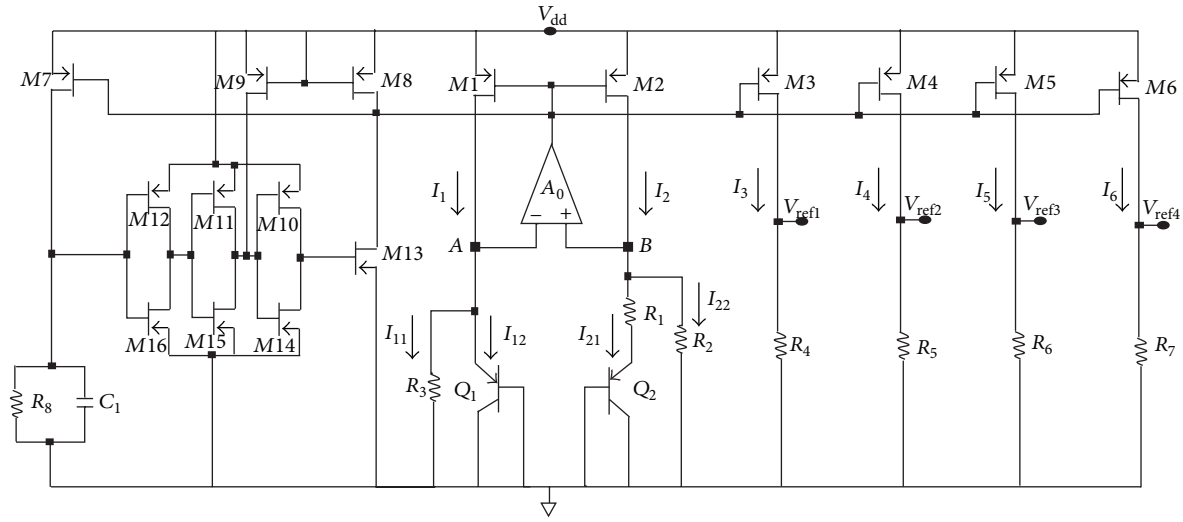

Figure 6: Bandgap reference multioutput.

V_{ref3}, and V_{ref4}), hence making use of multioutput bandgap reference tensions. Figure 6 shows a high precision temperature compensates CMOS bandgap reference [18]. This latter is improved in order to generate $V_{ref1} = 1.3$ V, $V_{ref2} = 1.4$ V, $V_{ref3} = 0.53$ mV, and $V_{ref4} = 0.99$ mV reference voltages by means of adding four out-stages.

The equation of the two generated currents, which are proportional to V_{EB} and ΔV_{EB}, to bias these four added stages, is the following equation:

$$I_1 = I_2 = \alpha I_3 = \beta I_4 = \gamma I_5 = \delta I_6. \tag{1}$$

As shown in Figure 6, each current is divided into two other currents passing through two branches containing resistor and bipolar transistor in such a way that

$$\begin{aligned} I_{11} &= I_{22}; \\ I_{12} &= I_{21}. \end{aligned} \tag{2}$$

We made $R_2 = R_3$, to make the voltage of A equal to B.

The inputs of the operational amplifier are equalized. From Figure 6, $V_A = V_{EB1}$. Consider

$$\begin{aligned} R_3 I_{11} &= R_2 I_{22}, \\ V_A &= V_B, \\ R_2 I_{22} &= V_A = V_B = V_{EB1}, \\ I_{22} &= \frac{V_{EB1}}{R_2}, \\ I_{21} R_1 &= V_B - V_{EB2} \\ &= V_A - V_{EB2} \\ &= V_{EB1} - V_{EB2} = \Delta V_{EB}, \\ I_{21} &= \frac{\Delta V_{EB}}{R_1}. \end{aligned} \tag{3}$$

So, the outputs reference voltages of the proposed multioutput BGR can be obtained as

$$\begin{aligned} V_{ref1} &= R_4 I_5 = \frac{R_4 I_2}{\alpha} \\ &= \frac{R_4 (I_{21} + I_{22})}{\alpha} \\ &= \frac{R_4}{\alpha} \left(\frac{\Delta V_{EB}}{R_1} + \frac{V_{EB1}}{R_2} \right), \\ V_{ref2} &= \frac{R_5}{\beta} \left(\frac{\Delta V_{EB}}{R_1} + \frac{V_{EB1}}{R_2} \right), \\ V_{ref3} &= \frac{R_6}{\gamma} \left(\frac{\Delta V_{EB}}{R_1} + \frac{V_{EB1}}{R_2} \right), \\ V_{ref4} &= \frac{R_7}{\delta} \left(\frac{\Delta V_{EB}}{R_1} + \frac{V_{EB1}}{R_2} \right). \end{aligned} \tag{4}$$

Unlike V_{EB1}, which has a negative TC, ΔV_{EB} has a positive TC. So, all outputs (V_{ref1}, V_{ref2}, V_{ref3}, and V_{ref4}) become almost autonomous from temperature. Figure 7 shows the simulation of these aforementioned output reference voltages as a function of temperature over the range −40°C to 120°C.

3.3. Current Sense. To sense the current on power transistor MP we have used the M_{cs} transistor in the current sense circuit shown in Figure 8 to make the voltage of V_{sd} of M_{cs}

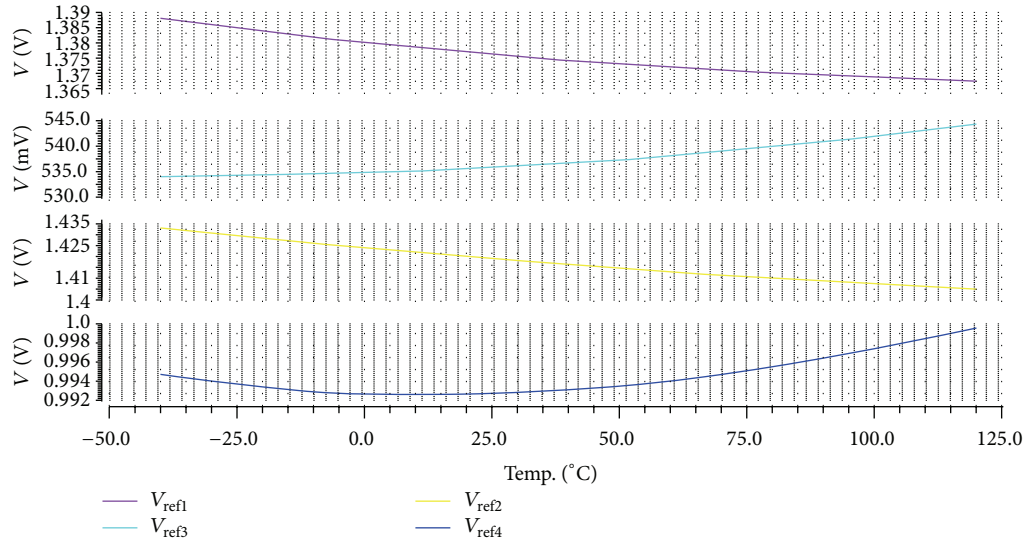

Figure 7: Reference voltages versus temperature.

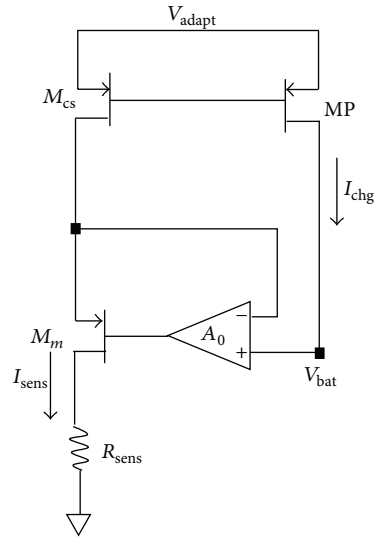

Figure 8: Current sense circuit.

and MP equal. We have used the OP. The current of M_{cs} MP can be described as the following equation:

$$\begin{aligned} I_{M_{cs}} &= \frac{1}{2}\mu_n C_{ox}\frac{W_{cs}}{L_{cs}}\left[2\left(V_{SG}-\left|V_{thp}\right|\right)V_{SD}-{V_{SD}}^2\right] \\ &= I_{sens}, \\ I_{MP} &= \frac{1}{2}\mu_n C_{ox}\frac{W_p}{L_p}\left[2\left(V_{SG}-\left|V_{thp}\right|\right)V_{SD}-{V_{SD}}^2\right] \\ &= I_{chg}. \end{aligned} \tag{5}$$

I_{chg} and I_{sens} are proportional to their aspect ratios. Their ratio can be described as

$$\frac{I_{sens}}{I_{chg}} \cong \frac{W_{cs}/L_{cs}}{W_p/L_p} = \frac{1}{N}. \tag{6}$$

Figure 9 shows the simulation results of sensing currents.

4. Simulation Results

The results simulation waveforms of the proposed Li-ion battery charger are presented in Figure 10. The reference

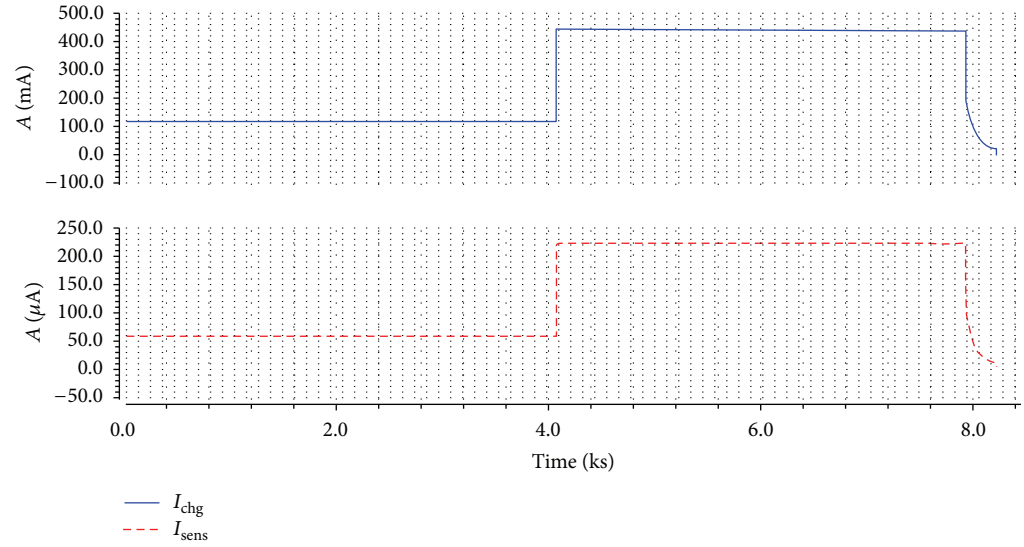

FIGURE 9: Simulation results of sensing currents; from top to bottom, the waveforms are the charging current I_{chg} and the sensed current I_{sens}, respectively.

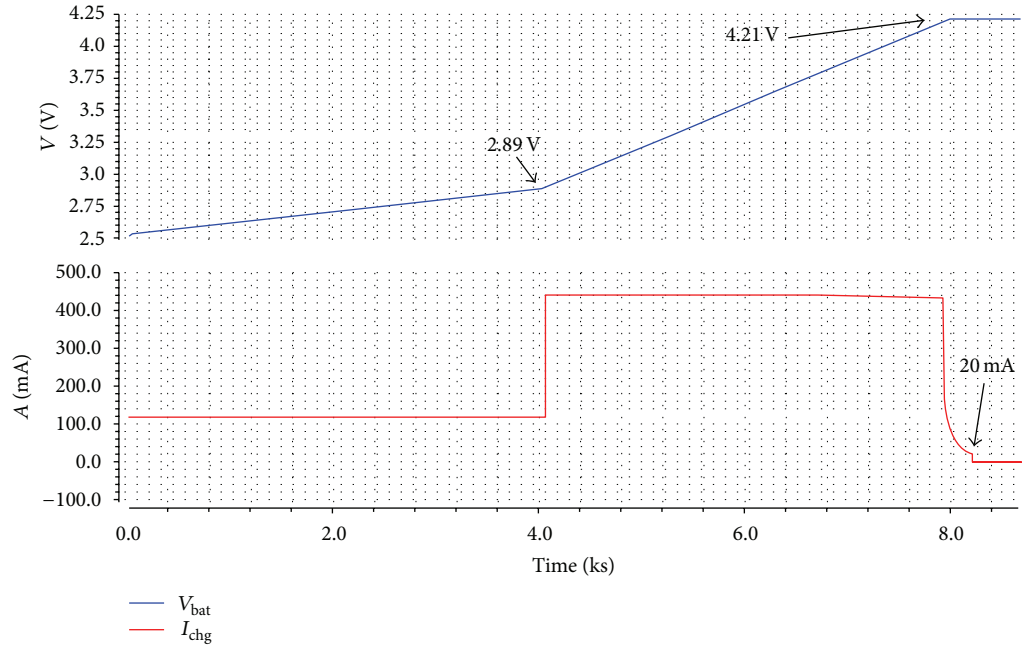

FIGURE 10: Simulation results of output voltage and current; from top to bottom, the waveforms are the battery voltage V_{batt} and the charging current I_{chg}, respectively.

currents are, respectively, 116 mA and 448 mA for working at the trickle constant current and fast constant current modes. The range voltages are presented as 2.5 V and 4.2 V, correspondingly. The stop current is 20 mA that is equal to around 1C/40 that we have defined. The transition between CC and CV mode occurs, as shown in Figure 11. And as can be observed in Figure 12, the system is stable.

Figure 13 shows a layout of the battery charger integrated circuit. As expected, the Li-ion battery charger was designed using 0.18 μm technology; most of the area is occupied by

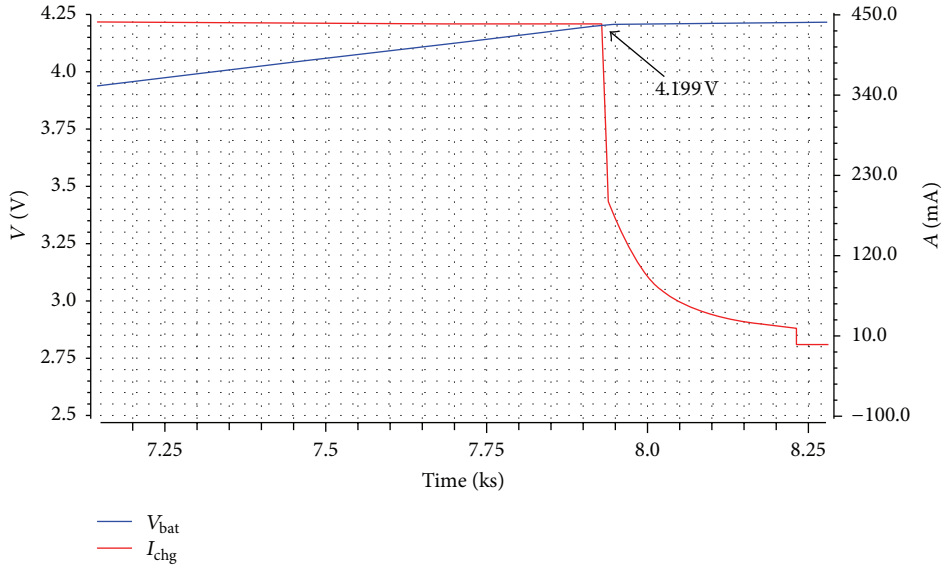

Figure 11: Transition from CC to CV mode.

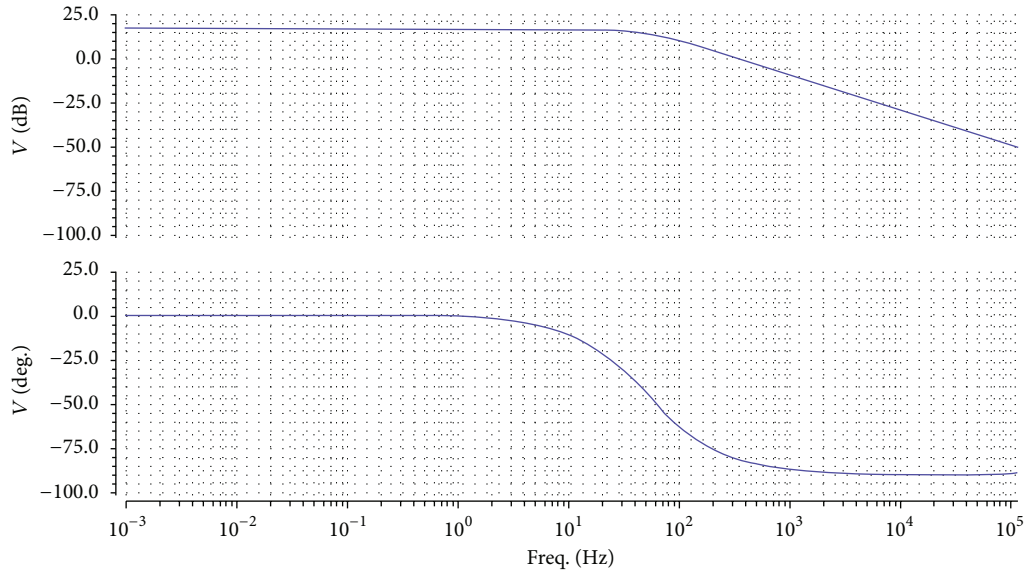

Figure 12: Frequency response of battery charger.

the power PMOS pass device, in which the effective die area is 1.172 mm^2.

Table 1 summarizes the performance characteristics of the proposed battery charger IC herein presented. Apparently, this work presents an average power efficiency up to 87% and better performance in terms of maximum current charge and very small chip size.

5. Conclusion

The presented Li-ion battery charger has been designed with 0.18 μm CMOS processes. The proposed charger is operating

Table 1: Summary of simulation results.

Topology	Adaptive LDO
Technology	0.18 μm
Supply voltage (V)	4.8–5
Efficiency (%)	87 at 4.8 V 84 at 5 V
Output voltage (V)	2.5–4.2
Maximum charging current	448 mA
Chip area	1.172 mm^2

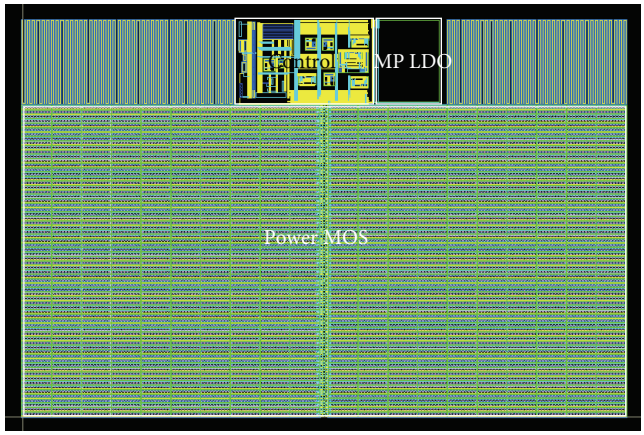

Figure 13: Layout of proposed charger.

within trickle constant current, fast constant current, and constant voltage triple mode with high power efficiency of 87%, small chip size, and low consumption and it is suitable for portable system as battery charger.

Conflict of Interests

The authors declare that there is no conflict of interests regarding the publication of this paper.

References

[1] M. Chen and G. A. Rincón-Mora, "Accurate, compact, and power-efficient li-ion battery charger circuit," *IEEE Transactions on Circuits and Systems II: Express Briefs*, vol. 53, no. 11, pp. 1180–1184, 2006.

[2] D. Linden and T. B. Reddy, *Handbook of Batteries*, chapter 35, McGraw-Hill, New York, NY, USA, 2002.

[3] Y.-S. Hwang, S.-C. Wang, F.-C. Yang, and J.-J. Chen, "New compact CMOS Li-ion battery charger using charge-pump technique for portable applications," *IEEE Transactions on Circuits and Systems I: Regular Papers*, vol. 54, no. 4, pp. 705–712, 2007.

[4] J. Buxton, "Li-ion battery charging requires accurate voltage sensing," *Analog Dialogue: Analog Devices*, vol. 31, no. 2, pp. 3–4, 1997.

[5] C.-H. Lin, C.-Y. Hsieh, and K.-H. Chen, "A Li-ion battery charger with smooth control circuit and built-in resistance compensator for achieving stable and fast charging," *IEEE Transactions on Circuits and Systems. I. Regular Papers*, vol. 57, no. 2, pp. 506–517, 2010.

[6] H.-Y. Yang, T.-H. Wu, J.-J. Chen, Y.-S. Hwang, and C.-C. Yu, "An omnipotent Li-Ion battery charger with multimode controlled techniques," in *Proceedings of the IEEE 10th International Conference on Power Electronics and Drive Systems (PEDS '13)*, pp. 531–534, April 2013.

[7] R. Pagano, M. Baker, and R. E. Radke, "A 0.18-μ monolithic li-ion battery charger for wireless devices based on partial current sensing and adaptive reference voltage," *IEEE Journal of Solid-State Circuits*, vol. 47, no. 6, pp. 1355–1368, 2012.

[8] F.-C. Yang, C.-C. Chen, J.-J. Chen, Y.-S. Hwang, and W.-T. Lee, "Hysteresis-current-controlled buck converter suitable for Li-ion battery charger," in *Proceedings of the International Conference on Communications, Circuits and Systems (ICCCAS '06)*, pp. 2723–2726, Guilin, China, June 2006.

[9] P. H. V. Quang, T. T. Ha, and J.-W. Lee, "A fully integrated multimode wireless power charger IC with adaptive supply control and built-in resistance compensation," *IEEE Transactions on Industrial Electronics*, vol. 62, no. 2, pp. 1251–1261, 2015.

[10] J.-J. Chen, F.-C. Yang, C.-C. Lai, Y.-S. Hwang, and R.-G. Lee, "A high-efficiency multimode Li-Ion battery charger with variable current source and controlling previous-stage supply voltage," *IEEE Transactions on Industrial Electronics*, vol. 56, no. 7, pp. 2469–2478, 2009.

[11] J. A. De Lima, "A compact and power-efficient CMOS battery charger for implantable devices," in *Proceedings of the 27th Symposium on Integrated Circuits and Systems Design (SBCCI '14)*, September 2014.

[12] P. Li and R. Bashirullah, "A wireless power interface for rechargeable battery operated medical implants," *IEEE Transactions on Circuits and Systems II: Express Briefs*, vol. 54, no. 10, pp. 912–916, 2007.

[13] S.-H. Yang, J.-W. Liu, and C.-C. Wang, "A single-chip 60-V bulk charger for series Li-ion batteries with smooth charge-mode transition," *IEEE Transactions on Circuits and Systems. I. Regular Papers*, vol. 59, no. 7, pp. 1588–1597, 2012.

[14] C.-C. Tsai, C.-Y. Lin, Y.-S. Hwang, W.-T. Lee, and T.-Y. Lee, "A multi-mode LDO-based Li-ion battery charger in 0.35μM CMOS technology," in *Proceedings of the IEEE Asia-Pacific Conference on Circuits and Systems (APCCAS '04)*, vol. 1, pp. 49–52, IEEE, December 2004.

[15] R. C. Cope and Y. Podrazhansky, "The art of battery charging," in *Proceedings of the 14th Annual Battery Conference on Applications and Advances*, pp. 233–235, IEEE, Long Beach, Calif, USA, January 1999.

[16] S. Dearborn, "Charging Li-ion batteries for maximum run times," *Power Electronics Technology*, vol. 31, no. 4, pp. 40–49, 2005.

[17] S. S. Bethi, K.-S. Lee, R. Veillette, J. Carletta, and M. Willett, "A temperature and process insensitive CMOS reference current generator," in *Proceedings of the IEEE 56th International Midwest Symposium on Circuits and Systems (MWSCAS '13)*, pp. 301–304, 2013.

[18] A. Dey and T. K. Bhattacharyya, "Design of a CMOS bandgap reference with low temperature coefficient and high power supply rejection performance," *International Journal of VLSI Design & Communication Systems*, vol. 2, no. 3, pp. 139–150, 2011.